

Exploiting Shared Knowledge from Non-COVID Lesions for Annotation-Efficient COVID-19 CT Lung Infection Segmentation

Yichi Zhang, Qingcheng Liao, Lin Yuan, He Zhu, Jiezhen Xing, and Jicong Zhang

Abstract—The novel Coronavirus disease (COVID-19) is a highly contagious virus and has spread all over the world, posing an extremely serious threat to all countries. Automatic lung infection segmentation from computed tomography (CT) plays an important role in the quantitative analysis of COVID-19. However, the major challenge lies in the inadequacy of annotated COVID-19 datasets. Currently, there are several public non-COVID lung lesion segmentation datasets, providing the potential for generalizing useful information to the related COVID-19 segmentation task. In this paper, we propose a novel relation-driven collaborative learning model for annotation-efficient COVID-19 CT lung infection segmentation. The network consists of encoders with the same architecture and a shared decoder. The general encoder is adopted to capture general lung lesion features based on multiple non-COVID lesions, while the target encoder is adopted to focus on task-specific features of COVID-19 infections. Features extracted from the two parallel encoders are concatenated for the subsequent decoder part. To thoroughly exploit shared knowledge between COVID and non-COVID lesions, we develop a collaborative learning scheme to regularize the relation consistency between extracted features of given input. Other than existing consistency-based methods that simply enforce the consistency of individual predictions, our method enforces the consistency of feature relation among samples, encouraging the model to explore semantic information from both COVID-19 and non-COVID cases. Extensive experiments on one public COVID-19 dataset and two public non-COVID datasets show that our method achieves superior segmentation performance compared with existing methods in the absence of sufficient high-quality COVID-19 annotations.

Index Terms—COVID-19, Computed Tomography, Lung Infection Segmentation, Few-shot Learning, Knowledge Transfer.

I. INTRODUCTION

SINCE the beginning of 2020, the novel coronavirus disease (COVID-19) has spread worldwide, seriously endangering human health. This severe disease has been declared as a public health emergency of international concern by the World Health Organization (WHO). Until the end of September 2020, COVID-19 has caused more than 1,000,000 deaths, posing an extremely serious threat and challenge to all countries.

As one of the most commonly used imaging methods, computed tomography (CT) plays an important role in the fight against COVID-19 [1], [2], [3]. Researchers have proved that CT images have strong ability to capture typical features like ground glass and bilateral patchy shadows of affected patients [4] and are shown to be more sensitive compared with standard viral nucleic acid detection using real-time polymerase chain reaction (RT-PCR) for the early diagnosis of COVID-19 infection [5]. Besides, CT images can provide visual evaluation of the extent of lung abnormalities and assist the process of prognostic [6].

In clinical practice, the segmentation of lung infections from CT volumes is an important component to assist in further assessment and quantification of the diseases [7]. Since manual contour delineation is time-consuming and laborious, and suffers from inter and intra-observer variabilities [8], it is of great significance to develop artificial intelligence-based approaches to assist in the automatic segmentation of COVID-19 infections. Recently, the unprecedented development in deep learning has showed significant improvements and achieved state-of-the-art performances in many medical

This work is supported by the National Key Research and Development Program of China (2016YFF0201002), the University Synergy Innovation Program of Anhui Province (GXXT-2019-044), and the National Natural Science Foundation of China (61301005). The first two authors contributed equally to this work.

Yichi Zhang, Qingcheng Liao and Jiezhen Xing are with School of Biological Science and Medical Engineering, Beihang University, Beijing, China.

Lin Yuan is with College of Biomedical Engineering, Taiyuan University of Technology, Taiyuan, China.

He Zhu is with School of Computer Science and Engineering, Beihang University, Beijing, China.

Jicong Zhang (corresponding author) is with School of Biological Science and Medical Engineering, Beihang University, Beijing, China, and with Hefei Innovation Research Institute, Beihang University, Hefei, China, and with Beijing Advanced Innovation Centre for Biomedical Engineering, Beijing, China, and with Beijing Advanced Innovation Centre for Big Data-Based Precision Medicine, Beijing, China.

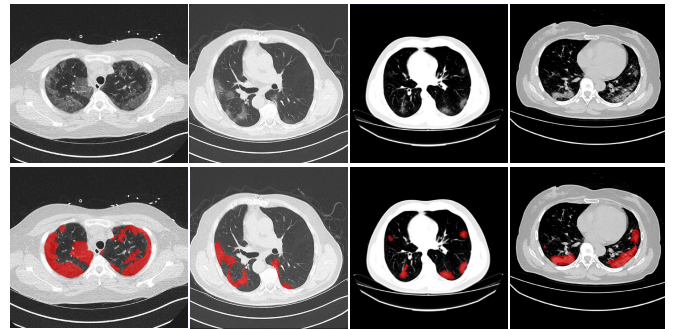


Fig. 1. Examples of COVID-19 CT cases showing the large variations of shape, size and position of lung infections. The upper row shows the raw image and the lower row shows corresponding annotation of infection areas.

image segmentation tasks [9], [10], [11], and deep neural networks have been widely applied in the global fight against COVID-19 [12], [13], [14], [15].

However, the success of deep learning methods mainly requires large amount of high-quality annotated datasets, while it is impractical to collect large amount of well annotated data in real clinical approach, especially when radiologists are busy fighting the coronavirus disease. Additionally, as shown in Fig.1, the large variations in shape, size and position of lung infections and large inter-case variations pose great challenges for the segmentation tasks [16]. Therefore, exploring annotation-efficient COVID-19 lung infection segmentation methods with limited labelled data has become an urgent need especially in the current situation.

Currently, there are several public non-COVID lung lesion datasets due to other clinical practices, such as MSD Lung for segmentation of lung tumor and NSCLC Pleural Effusion for segmentation of pleural effusion. These non-COVID datasets may serve as potential profit for generalizing useful information to the related COVID-19 infection segmentation task. Wang *et al.* [17] have proven that pre-training on non-COVID datasets can improve the segmentation performance of COVID-19 infection segmentation. However, the improvement of transfer learning is not stable when encountering large domain difference between datasets, and shared knowledge between COVID-19 and non-COVID lung lesions cannot be fully exploited.

To address these challenges, we propose a novel relation-driven collaborative learning model for annotation-efficient COVID-19 CT lung infection segmentation by exploiting shared knowledge from non-COVID lesions. The network consists of encoders with the same architecture and a shared decoder. The general encoder is adopted to capture general lung lesion features based on multiple non-COVID lesions, while the target encoder is adopted to focus on task-specific features of COVID-19 infections. Features extracted from the two parallel encoders are concatenated for the subsequent decoder part. Besides, we develop a collaborative learning scheme to exploit shared knowledge between COVID and non-COVID lesions by regularizing the relation consistency between extracted features of given input. Our method can enforce the consistency of feature relation among different samples and encourage the model to explore semantic information from both COVID-19 and non-COVID cases. The contributions of this work are summarized as follows:

- We propose a novel relation-driven collaborative learning model for annotation-efficient segmentation of COVID-19 lung infections from CT volumes by leveraging shared knowledge from non-COVID lesions to improve the segmentation performance of COVID-19 infections with limited training data.
- We present a collaborative learning scheme to explore general semantic information from both COVID-19 and non-COVID cases by regularizing the relation consistency between extracted features of given input, so as to encourage the model to learn more general and discriminative representation of COVID-19 infections for better segmentation performance.

- We have conducted extensive experiments on one COVID-19 dataset and two non-COVID lung lesion datasets. The results show that our method achieves superior segmentation performance compared with other methods in the absence of sufficient high-quality COVID-19 data.

II. RELATED WORK

In this section, we briefly review the research related to our work. We first review works on annotation-efficient deep learning for medical image segmentation. Then we review existing works on COVID-19 segmentation and transfer learning approaches for COVID-19.

A. Annotation-efficient Deep Learning

Compared with natural images, the annotations of medical images are much harder and more expensive to acquire due to following problems: 1) annotating medical images heavily relies on professional diagnosis knowledge of radiologists; 2) most modalities of medical images like CT are 3D volumes, which will take much more time and labor for annotation. To alleviate annotation scarcity, annotation-efficient methods have received great attention in medical image analysis community [18], [19]. For example, semi-supervised learning aims at learning from a limited amount of labeled data and a large amount of unlabeled data, which is an effective way to explore knowledge from the unlabeled data [20]. Weakly supervised learning explores the use of weak annotations like noisy annotations and sparse annotations [21]. Besides, some approaches also aim at integrating multiple related datasets to learn general knowledge [22], [23]. To issue the problem of limited labeled COVID-19 data, in this work, we aim at utilizing existing non-COVID lung lesion datasets for generalizing useful information to related COVID-19 task, so as to achieve better segmentation performance with limited in-domain training data.

B. Research on COVID-19 Segmentation

Automatic segmentation of COVID-19 infections from CT volumes is a crucial step to for quantification of the disease progression. Recently, several approaches have been proposed for COVID-19 lung infection segmentation. Shan *et al.* [24] propose a deep learning-based system for automatic segmentation and quantification of infection regions. Amyar *et al.* [25] propose to improve the segmentation performance with a multi-task learning approach. Other than fully supervised learning, Zheng *et al.* [26] develop a weakly-supervised approach to investigate the potential for automatic detection of COVID-19 based on patient-level label. Fan *et al.* [27] present a lung infection segmentation network for 2D CT slices with semi-supervised strategy. Wang *et al.* [28] propose a noise-robust framework to learn from noisy labels for the pneumonia lesion segmentation task. Yao *et al.* [29] use a set of operations to synthesize lesion-like appearances for label-free segmentation.

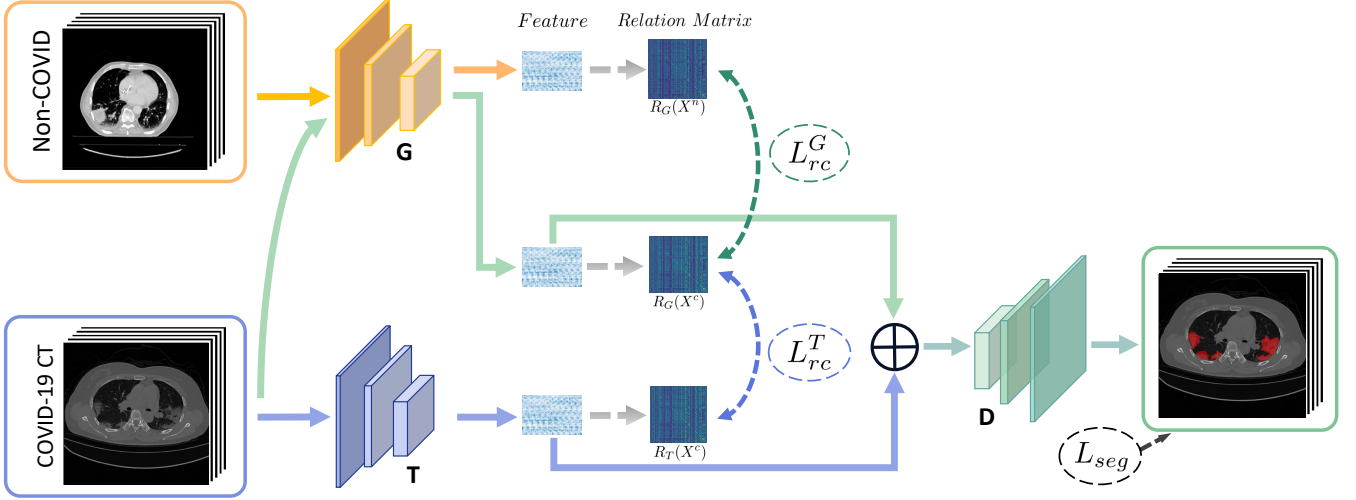


Fig. 2. The overview of our proposed relation-driven collaborative learning model, where green and blue represent the data flow of general encoder and target encoder for COVID-19 infection segmentation, respectively. Extracted features from these two parallel encoders are concatenated for the input of the shared decoder. To exploit shared knowledge from non-COVID-cases, an additional data flow in orange is adopted. By regularizing the relation consistency between extracted features of given input, the model is encouraged to explore semantic information from both COVID-19 and non-COVID cases.

C. Transfer Learning Approaches for COVID-19

Transfer learning aims to leverage knowledge and latent features from other datasets by pre-training models on large datasets and fine-tuning trained models on downstream tasks. Due to the problem of limited COVID-19 data, several transfer learning methods have been applied. For example, Wang *et al.* Chouhan [30] propose an ensemble model to combine outputs from five pre-trained models based on ImageNet. Majeed *et al.* [31] adopt transfer learning procedure and propose a simple CNN architecture with a small number of parameters to distinguish COVID-19 from normal X-rays. Misra *et al.* [32] propose a multi-channel pre-trained ResNet architecture to facilitate the diagnosis of COVID-19. For segmentation of COVID-19 infections, Wang *et al.* [17] evaluate different transfer learning methods and revealed the benefits of transferring knowledge from non-COVID lung lesions. However, transfer learning only takes the advantage of existing models, and non-COVID cases are not utilized in the training procedure of downstream COVID-19 segmentation tasks. Different from these existing methods, our method aims at learning from COVID-19 and non-COVID lung lesions collaboratively to exploit shared semantic information.

III. METHOD

In this section, we first introduce the overview of our proposed method. Then we provide details of our relation-driven collaborative learning scheme and the overall training procedure.

A. Overview

An overview of our proposed framework is shown in Fig2. Following the design of standard U-Net [33], [34], our network

consists of two encoders with the same architecture and a shared decoder. Since the encoder serves as a contraction to extract image contextual features, the upper one named general encoder (G) is adopted to capture general lung lesion features based on multiple non-COVID lesions, and the lower one named target encoder (T) is adopted to focus on task-specific features of the target COVID-19 infection segmentation task. After that, extracted features from these two parallel encoders are concatenated together for the input of the decoder. The shared decoder (D) serves as a symmetric expanding path to recover the spatial information of the extracted features. The skip connections between the target encoder and shared decoder are employed for the fusion of multi-scale features.

Given a set of samples $\{X_i^c, Y_i^c\}_{i=1}^{N_c}$ from COVID-19 datasets S_c and a set of samples $\{X_i^n, Y_i^n\}_{i=1}^{N_n}$ from non-COVID datasets S_n , where X and Y denote the CT volume and corresponding annotation of lung lesions. For the segmentation workflow, the general encoder is applied to extract general features, while the target encoder is applied to extract the task-specific features. These extracted features are concatenated and then fed into the decoder part to get the final segmentation results. To issue the problem of limited COVID-19 training data, instead of transferring pre-trained models to the downstream learning task of X^n , we aim to involve X^c collaboratively in the training procedure of COVID-19 to exploit shared knowledge from non-COVID cases, which can be used as a guidance for the learning of target COVID-19 infection segmentation. Specifically, a relation-driven collaborative learning scheme is applied to regularize the relation consistency between extracted features of given input and encourage the model to explore semantic information.

B. Relation-driven Collaborative Learning

Inspired by recent study on relational-driven semi-supervised learning [35], we aim to exploit shared knowledge from non-COVID lesions by regularizing the relation consistency between extracted features of given input, so as to facilitate the learning procedure of COVID-19 infections. Based on the assumption that general encoder is adopted to capture general features of lung lesion, and the target encoder is adopted to focus on task-specific COVID-19 infection features, we propose to utilize the relation of features extracted from these two encoders as guidance for the collaborative learning approach.

To estimate the feature relation, we model the feature relation with channel-wise Gram Matrix [36]. For each input batch with B samples, we average the features within each batch to get the mean representation. We denote the extracted feature maps of encoder $F \in R^{C \times H \times W \times D}$, where H , W and D represent the spatial dimension of feature maps, and C represents the channel number. To obtain channel-wise feature relation, we reshape the feature maps into $A \in R^{C \times HWD}$. After that, we get the channel-wise Gram Matrix as follows:

$$G = A \cdot (A)^T \quad (1)$$

where G_{mn} is the inner product between the vectorized activation map of $A_{(m)}$ and $A_{(n)}$, representing the similarity between the m_{th} and n_{th} channel. The final feature relation matrix R is obtained by conducting the L2 normalization for each row of G as follows:

$$R = [\frac{G_1}{\|G_1\|_2}, \dots, \frac{G_C}{\|G_C\|_2}]^T \quad (2)$$

After the modeling of feature relation, our method regularizes the network to learn more general and discriminative representation of COVID-19 infections by regularizing the feature relation consistency among given input, thereby encouraging the network to explore semantic information from both COVID-19 and non-COVID cases.

For explicit learning, the network is optimized based on the supervised segmentation loss L_{seg} between output \hat{Y}^c and corresponding ground truth Y^c . We use the combination of dice loss L_{dice} and cross entropy loss L_{ce} as the supervised segmentation loss, and deep supervision [37] is applied to obtain multi-scale supervision at different scales. The segmentation loss can be summarized as

$$L_{seg} = L_{dice}(\hat{Y}^c, Y^c) + L_{ce}(\hat{Y}^c, Y^c) \quad (3)$$

Besides, to utilize the feature relation for collaborative learning, the non-COVID cases are additionally fed into general encoder to explore the general feature representation and its corresponding feature relation matrix $R_G(X^n)$. The proposed scheme requires the generated feature relation matrices of general encoder to be stable using general relation consistency loss L_{rc}^G defined as:

$$L_{rc}^G = \sum_{\{X^n, X^c\} \in \{S_n, S_c\}} \lambda_G \|R_G(X^n) - R_G(X^c)\|^2 \quad (4)$$

Algorithm 1 Training procedure of our proposed framework.

Input: A batch of (X^c, Y^c) from COVID-19 dataset D_c and (X^n, Y^n) from non-COVID dataset D_n .

Output: Trained network N with parameters $\theta_G, \theta_T, \theta_D$

- 1: **while** not converge **do**
 - 2: $(X^c, Y^c), (X^n, Y^n) \leftarrow$ sampled from D_c and D_n
 - 3: Generate features of general encoder $F_G(X^c)$ and target encoder $F_T(X^c)$
 - 4: Generate general feature representation $F_G(X^n)$
 - 5: Calculate feature relation matrices $R_G(X^c)$, $R_T(X^c)$ and $R_G(X^n)$ as Eq. (1) and (2)
 - 6: Generate segmentation output \hat{Y}^c
 - 7: Calculate segmentation loss L_{seg} as Eq. (3)
 - 8: Calculate consistency losses L_{rc}^G, L_{rc}^T as Eq. (4) and (5)
 - 9: Update θ_T, θ_D with L_{seg}
 - 10: Update θ_G with L_{rc}^G
 - 11: Update θ_T with L_{rc}^T
 - 12: Ramp up the weighting coefficients λ_G and λ_T
 - 13: **end while**
 - 14: **return** Trained network N
-

while for target encoder, the extracted target-specific feature relation matrices are enforced to be more discriminative using target relation consistency loss L_{rc}^T defined as:

$$L_{rc}^T = \sum_{\{X^n, X^c\} \in \{S_n, S_c\}} -\lambda_T \|R_G(X^c) - R_T(X^c)\|^2 \quad (5)$$

where $R_G(X^c)$ and $R_T(X^c)$ denote the feature relation matrices of COVID-19 cases extracted from general encoder and target encoder, respectively. λ_G and λ_T are ramp-up weighting coefficients that control the trade-off between the segmentation loss and consistency loss, so as to mitigate the disturbance of consistency loss at early training stage.

Since the network is supervised by limited COVID-19 cases, the training may become unstable and with poor generalization ability. By minimizing feature relation consistency losses L_{rc}^G and L_{rc}^T during the training procedure, the general encoder and target encoder can be enhanced to capture more general and discriminative representation, thereby exploring useful shared knowledge from adequate non-COVID data for better segmentation performance.

C. Overall Training Procedure

Algorithm1 presents the detailed training procedure of our framework. For the optimization of the network, we update the target encoder and decoder based on the supervised segmentation loss L_{seg} . Besides, relation consistency losses L_{rc}^G and L_{rc}^T are used to update the general encoder and target encoder, respectively. The collaborative learning scheme allow the two parallel encoders to benefit from each other's guidance, encouraging the model to explore semantic information from both COVID-19 and non-COVID cases.

TABLE I

DETAILS OF 3D U-NET ARCHITECTURE USED IN OUR EXPERIMENTS. NOTE THAT THE GENERAL ENCODER AND TARGET ENCODER ARE WITH THE SAME ARCHITECTURE AS SHOWN IN THE LEFT COLUMN.

feature size	encoder (G / T)		decoder (D)	
1x56x160x192	input		output	conv(1x1x1)-sigmoid
32x56x160x192	conv1	conv(1x3x3)-IN-LReLU	conv10	conv(1x3x3)-IN-LReLU
64x56x80x96	down1	strided conv(1,2,2)	up10	transposed conv(1,2,2) - conv1
64x56x80x96	conv2	conv(3x3x3)-IN-LReLU	conv9	conv(3x3x3)-IN-LReLU
128x28x40x48	down2	strided conv(2,2,2)	up9	transposed conv(2,2,2) - conv2
128x28x40x48	conv3	conv(3x3x3)-IN-LReLU	conv8	conv(3x3x3)-IN-LReLU
256x14x20x24	down3	strided conv(2,2,2)	up8	transposed conv(2,2,2) - conv3
256x14x20x24	conv4	conv(3x3x3)-IN-LReLU	conv7	conv(3x3x3)-IN-LReLU
320x7x10x12	down4	strided conv(2,2,2)	up7	transposed conv(2,2,2) - conv4
320x7x10x12	conv5	conv(3x3x3)-IN-LReLU	conv6	conv(3x3x3)-IN-LReLU
320x7x5x6	down5	strided conv(1,2,2)	up6	transposed conv(1,2,2) - conv5

IV. EXPERIMENTS

A. Dataset Introduction

1) *COVID-19 Dataset*: This dataset is released by Coronacases Initiative and Radiopaedia and contains 20 COVID-19 CT volumes, which is publicly available at¹. The annotation of infections is labeled by two radiologists and verified by an experienced radiologist by Ma *et al.* [38].

2) *Non-COVID Lung Lesion Datasets*: In order to explore relevant information from non-COVID lung lesions to promote the annotation-efficient training of COVID-19 cases, we select out two public non-COVID lung lesion segmentation datasets for our following experiments. The first dataset is MSD Lung Tumor Dataset of Medical Segmentation Decathlon (MSD) Challenge [39] in MICCAI 2018². This dataset is comprised of patients with non-small cell lung cancer from Stanford University (Palo Alto, CA, USA) publicly available through TCIA. The tumor is annotated by an expert thoracic radiologist and 63 labeled CT volumes are used. The second dataset is NSCLC Pleural Effusion Dataset³. This dataset contains 78 CT volumes with annotation of pleural effusion. To exploit general features of lung lesions, we combine MSD and NSCLC datasets to form a non-COVID multi-lesion dataset in the following experiments.

B. Experimental Settings and Implementation Details

All the experiments in our work are implemented in Pytorch [40] and trained on NVIDIA Tesla V100 GPUs. To make a fair comparison, we follow the task settings of COVID-19 benchmarks in [38]. For the COVID-19 dataset, we make 5-fold cross validation based on pre-defined dataset split. Each fold contains 4 scans (20%) for training and 16 scans (80%) for testing. For non-COVID lung lesion datasets, we randomly

select 80% of the data for training and the rest of 20% for validation.

We use 3D U-Net [34] as the backbone network with nnU-Net implementation [41]. Since nnU-Net can automatically adapt preprocessing strategies and network architectures based on the analysis of given dataset, to unify the setting for our collaborative learning approach, we manually adjust the patch size and network architectures to the design of target COVID-19 infection segmentation task. The input patch size is set as 56x160x192 with batch size of 2. Stochastic gradient descent (SGD) optimizer is used for training with initial learning rate of 0.01 and momentum of 0.99. The detailed structure of the network is shown in Table I.

Motivated by the evaluation methods of the medical image segmentation decathlon [39], we employ two complementary metrics to evaluate the segmentation performance. Dice Similarity Coefficient (DSC), a region-based measure is used to measure the region mismatch, and Normalized surface Dice (NSD), a boundary-based measure is used to evaluate how close the segmentation and ground truth surfaces are to each other. Both metrics take the values in [0,1] and higher scores represent better segmentation performance. Let G and S denote the ground truth and the segmentation result, respectively. The two metrics are defined as follows:

$$DSC(G, S) = \frac{2|G \cap S|}{|G| + |S|}; \quad (6)$$

$$NSD(G, S) = \frac{|\partial G \cap B_{\partial S}^{(\tau)}| + |\partial S \cap B_{\partial G}^{(\tau)}|}{|\partial G| + |\partial S|}. \quad (7)$$

where $B_{\partial G}^{(\tau)}, B_{\partial S}^{(\tau)}$ denote the border regions of ground truth and segmentation surface at a threshold τ to tolerate the inter-rater variability of the annotators. We set $\tau = 3\text{mm}$ for the evaluation of segmentation results in the following experiments.

¹<https://zenodo.org/record/3757476#.X4ABeYvivid>

²<http://medicaldecathlon.com/>

³<https://wiki.cancerimagingarchive.net/display/Public/NSCLC-Radiomics>

TABLE II
QUANTITATIVE RESULTS OF 5-FOLD CROSS VALIDATION OF ABLATION ANALYSIS IN OUR EXPERIMENTS.

Method	DSC						NSD					
	Fold 0	Fold 1	Fold 2	Fold 3	Fold 4	Avg	Fold 0	Fold 1	Fold 2	Fold 3	Fold 4	Avg
nnUNet Baseline	0.681	0.713	0.662	0.681	0.627	0.673 ± 0.223	0.709	0.718	0.717	0.708	0.649	0.700 ± 0.224
Ours (backbone)	0.689	0.721	0.712	0.720	0.632	0.695 ± 0.205	0.709	0.747	0.770	0.764	0.649	0.728 ± 0.216
Ours (L_{rc}^G)	0.701	0.727	0.727	0.710	0.625	0.699 ± 0.210	0.747	0.758	0.790	0.763	0.648	0.740 ± 0.221
Ours ($L_{rc}^G + L_{rc}^T$)	0.723	0.728	0.718	0.720	0.625	0.703 ± 0.193	0.756	0.760	0.790	0.771	0.631	0.742 ± 0.203

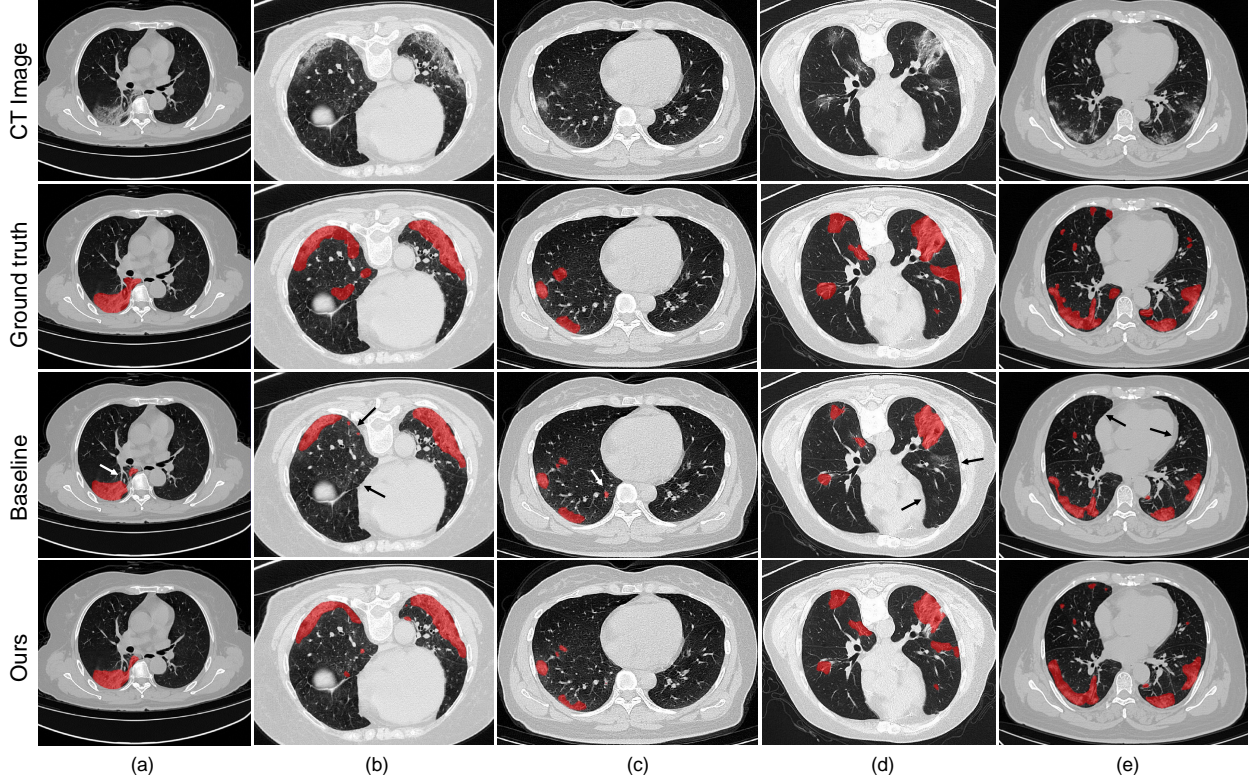


Fig. 3. Visual comparison of COVID-19 infection segmentation results by different methods. As we can see, our method can generate segmentation results with more accurate boundaries and less segmentation mistakes in small infection areas, which is closer to the ground truth.

C. Ablation Analysis

To investigate the effectiveness of the key components in our framework, we conduct ablation studies by removing the feature relation consistency loss. As shown in Table II, it is observed that all our methods can achieve better performance on all metrics compared with baseline results, showing the effectiveness of our method. When removing the target relation consistency, the average segmentation performance of five folds are degraded by 0.4% and 0.2% on DSC and NSD, respectively. The result proves that the usage of target relation consistency loss L_{rc}^T can enforce the target encoder to be more discriminative, so as to improve the segmentation performance. However, the improvement is susceptible to the domain difference. Besides, we also conduct experiments of our backbone by removing the general relation consistency loss. In this way, the general encoder is frozen and are not

updated during the training procedure, which means that the knowledge transfer is not available. The experimental results demonstrate that the average segmentation performance are degraded by 0.8% and 1.4% on DSC and NSD, showing the importance of knowledge transfer in our collaborative learning scheme.

D. Comparison Experiments with State-of-the-art Methods

To demonstrate the effectiveness of our method, we conduct extensive comparison experiments with other state-of-the-art methods. To ensure a fair comparison, all methods are experimented with the same network backbone and experimental settings. Segmentation models trained from scratch with only COVID-19 cases serve as our baseline results. Besides, as a simple and intuitive approach, pre-training segmentation models on non-COVID cases and fine-tuning on COVID-19

TABLE III
QUANTITATIVE RESULTS OF 5-FOLD CROSS VALIDATION OF COMPARISON EXPERIMENTS WITH STATE-OF-THE-ART METHODS. THE BEST RESULTS ARE SHOWN IN RED FONT AND THE SECOND BEST RESULTS IN BLUE FONT.

Method	DSC						NSD					
	Fold 0	Fold 1	Fold 2	Fold 3	Fold 4	Avg	Fold 0	Fold 1	Fold 2	Fold 3	Fold 4	Avg
nnUNet baseline	0.681	0.713	0.662	0.681	0.627	0.673±0.223	0.709	0.718	0.717	0.708	0.649	0.700±0.224
Pre-train on MSD	0.679	0.706	0.724	0.708	0.623	0.688±0.201	0.706	0.708	0.785	0.724	0.642	0.713±0.225
Pre-train on NSCLC	0.696	0.716	0.673	0.690	0.579	0.671±0.228	0.714	0.720	0.734	0.707	0.590	0.693±0.248
Ours (best)	0.723	0.728	0.718	0.720	0.625	0.703±0.193	0.756	0.760	0.790	0.771	0.631	0.742±0.203
Pre-train on Multi-lesion*	0.702	0.736	0.703	0.725	0.612	0.696±0.213	0.715	0.730	0.755	0.754	0.628	0.717±0.227
Multi-encoder* [17]	0.712	0.732	0.721	0.742	0.608	0.703±0.201	0.735	0.740	0.785	0.772	0.629	0.732±0.218

Note: * denotes the method use additional non-COVID datasets.

cases are utilized as comparison results for learning from both COVID-19 and non-COVID cases. The quantitative experimental results are shown in Table III. From the results, we can observe that transferring pre-trained models to COVID-19 infection segmentation tasks can generally improve the performance of training from scratch with only COVID-19 cases on most experiments, and using multi-lesion is superior to single-lesion when more general representations can be utilized to help COVID-19 infection tasks, with 2.3% and 1.7% improvements in DSC and NSD, respectively. However, these transfer learning methods show instability under different data distribution in five-fold cross validation experiments. The rationale is that the transfer ability largely depends on the domain difference between datasets. When there exists a large domain distance between non-COVID and limited COVID-19 training cases, transfer learning may somehow mislead the learning procedure.

In [17], the authors propose a multi-encoder architecture to freeze the non-COVID pre-trained encoder as an additional feature extractor for the training of COVID-19 cases. Features from the frozen adapted-encoder and reinitialized self-encoder are concatenated for the subsequent decoder. However, their workflow is still based on transfer learning, that training a network first on non-COVID cases and then on COVID-19 cases with foregoing pre-trained parameters. The main limitation is that the learning procedures of two tasks are separate. Therefore, the shared knowledge of non-COVID and COVID-19 cases cannot be exploited. It is observed that our method takes advantage of collaborative learning between two encoders and interactively improves the overall learning procedure. As a consequence, our method achieves the highest segmentation performance with an averaged DSC of 70.3% and averaged NSD of 74.2%. Visual comparison of segmentation results is shown in Fig.3. As shown in the figure, our method can generate segmentation results with more accurate boundaries in Fig.3(a)(b), and less segmentation mistakes in small infection areas in Fig.3(c)(d)(e). These results demonstrate that the collaborative learning approach can better exploit shared knowledge from non-COVID cases, leading to better performance when generalizing on test data.

E. Visual Analysis of Our Method

To better analysis the learning procedure and validate the effectiveness of our method, we show some visual examples of feature relation matrices at different epochs during the network training procedure in Fig.4 and Fig.5. The absolute differences of these two matrices are shown in the right column in red to clearly visualize the alignment of matrices. It can be observed in Fig.4 that as the training goes on, the network gradually produces more meaningful relation matrices with higher response at the same channel. Meanwhile, the absolute differences of feature relation matrices extracted from general encoder are gradually decreased, indicating that the general encoder learns more general and robust representations of lung lesions. Besides, as observed in Fig.5, the absolute differences of general and target feature relation matrices gradually increase and tend to be stable, indicating that the target encoder is gradually enforced to be more discriminative.

V. DISCUSSION

With the outbreak of COVID-19 all over the world, designing effective automated tools for fighting against COVID-19 is highly demanded to improve the efficiency of clinical approaches and reduce the tedious workload of clinicians and radiologists. However, accurate segmentation of COVID-19 lung infections is a challenging task due to the large appearance variance of COVID-19 lesions of patients in different severity level, and existing data-driven segmentation methods mainly rely on large amount of well annotated data. In order to mitigate the insufficiency of labeled COVID-19 CT scans, it is essential and meaningful to develop annotation-efficient segmentation methods for the COVID-19 lung infection segmentation task.

Considering that there are several public non-COVID lung lesion segmentation datasets due to other clinical practice, these datasets may serve as potential profit for generalizing useful information to assist in the related COVID-19 infection segmentation task. Some previous studies also highlight the usage of non-COVID lung lesions [17], [38]. However, these existing approaches merely focus on investigating the transferability in COVID-19 infection segmentation. Although their results reveal benefits of pre-training on non-COVID

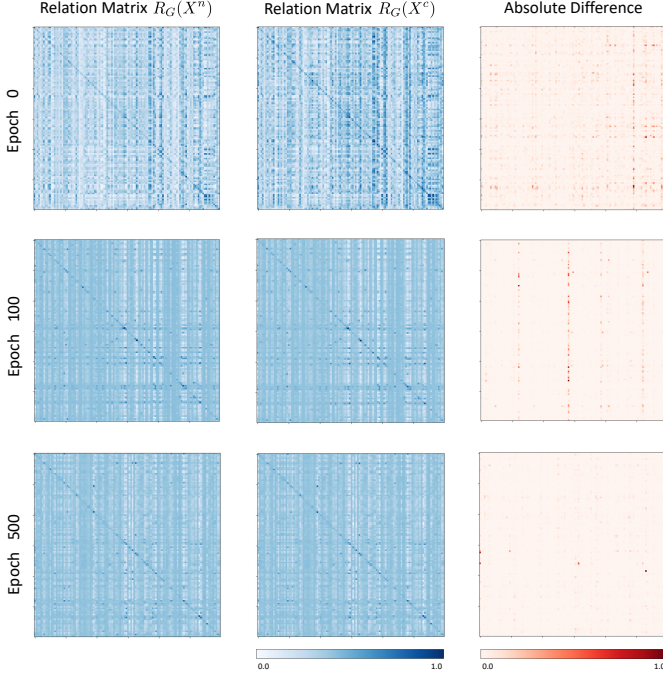


Fig. 4. Visualization of the general feature relation matrices of non-COVID cases (left column) and COVID-19 cases (middle column) and their absolute difference (right column) during the training procedure.

datasets, the improvement is limited when shared knowledge between COVID-19 and non-COVID lung lesions cannot be fully utilized. Our experiment reveal that the proposed collaborative learning scheme can effectively exploit shared semantic information by regularizing the consistency between extracted features so as to promote the training procedure in the absence of sufficient high-quality COVID-19 data.

Although promising performance has been achieved for learning from non-COVID lesions, the limitation of our method still exists. Due to the limitation of data, we only evaluate our method on two non-COVID datasets and one relatively small COVID-19 dataset. As a near future work, we plan to extend our method to more diverse datasets with larger amount of multi-institutional, multi-national cases like [42] to further enhance the generalization capability of our model for COVID-19 lung infection segmentation in the absence of sufficient annotations. In addition, we also plan to extend our method to other related medical image segmentation tasks to explore the usage of existing annotations effectively, thus enhancing the applicability of deep learning methods in real-world applications.

VI. CONCLUSION

In this paper, we propose a novel multi-lesion collaboratively learning model to exploit shared knowledge from non-COVID lesions for annotation-efficient COVID-19 lung infection segmentation from CT volumes. In specific, the network consists of encoders with the same architecture and a shared decoder. The general encoder is adopted to capture general lung lesion features based on multiple non-COVID lesions and the target encoder is adopted to focus on task-

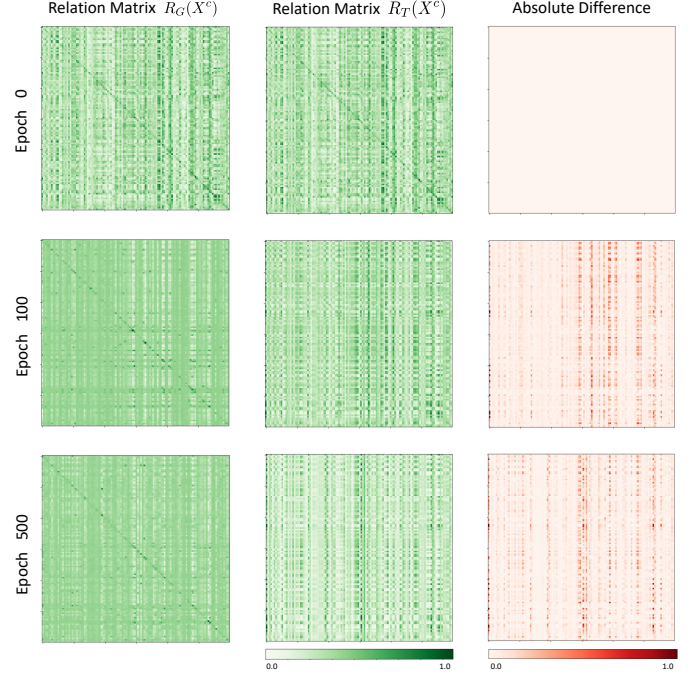


Fig. 5. Visualization of the general feature relation matrix (left column) and target feature relation matrix (middle column) of COVID-19 cases and their absolute difference (right column) during the training procedure.

specific feature of target COVID-19 infection. Besides, we develop a collaborative learning scheme to exploit shared knowledge from non-COVID lesions by regularizing the relation consistency between extracted features of given input. Experimental results on two non-COVID datasets and one COVID-19 dataset demonstrate the superiority of our method over existing state-of-the-art methods in the absence of sufficient high-quality annotations, illustrating strong potential for real-world applications in the global fight against COVID-19.

REFERENCES

- [1] P. J. Mazzone, M. K. Gould, D. A. Arenberg, A. C. Chen, H. K. Choi, F. C. Detterbeck, *et al.*, “Management of lung nodules and lung cancer screening during the covid-19 pandemic: Chest expert panel report,” *Chest*, 2020.
- [2] M. Oudkerk, H. R. Büller, D. Kuijpers, N. van Es, S. F. Oudkerk, T. C. McLoud, *et al.*, “Diagnosis, prevention, and treatment of thromboembolic complications in covid-19: report of the national institute for public health of the netherlands,” *Radiology*, p. 201629, 2020.
- [3] Y. Li and L. Xia, “Coronavirus disease 2019 (covid-19): role of chest ct in diagnosis and management,” *American Journal of Roentgenology*, vol. 214, no. 6, pp. 1280–1286, 2020.
- [4] M. Chung, A. Bernheim, X. Mei, N. Zhang, M. Huang, X. Zeng, *et al.*, “Ct imaging features of 2019 novel coronavirus (2019-ncov),” *Radiology*, vol. 295, no. 1, pp. 202–207, 2020.
- [5] Y. Fang, H. Zhang, J. Xie, M. Lin, L. Ying, P. Pang, *et al.*, “Sensitivity of chest ct for covid-19: comparison to rt-pcr,” *Radiology*, p. 200432, 2020.
- [6] K. Li, Y. Fang, W. Li, C. Pan, P. Qin, Y. Zhong, *et al.*, “Ct image visual quantitative evaluation and clinical classification of coronavirus disease (covid-19),” *European Radiology*, pp. 1–10, 2020.
- [7] F. Shi, J. Wang, J. Shi, Z. Wu, Q. Wang, Z. Tang, *et al.*, “Review of artificial intelligence techniques in imaging data acquisition, segmentation and diagnosis for covid-19,” *IEEE Reviews in Biomedical Engineering*, 2020.
- [8] L. Joskowicz, D. Cohen, N. Caplan, and J. Sosna, “Inter-observer variability of manual contour delineation of structures in ct,” *European Radiology*, vol. 29, no. 3, pp. 1391–1399, 2019.

- [9] P. Bilic, P. F. Christ, E. Vorontsov, G. Chlebus, H. Chen, Q. Dou, *et al.*, “The liver tumor segmentation benchmark (lits),” *arXiv preprint arXiv:1901.04056*, 2019.
- [10] N. Heller, F. Isensee, K. H. Maier-Hein, X. Hou, C. Xie, F. Li, *et al.*, “The state of the art in kidney and kidney tumor segmentation in contrast-enhanced ct imaging: Results of the kits19 challenge,” *Medical Image Analysis*, vol. 67, p. 101821, 2019.
- [11] O. Bernard, A. Lalande, C. Zotti, F. Cervenansky, X. Yang, P.-A. Heng, *et al.*, “Deep learning techniques for automatic mri cardiac multi-structures segmentation and diagnosis: is the problem solved?” *IEEE Transactions on Medical Imaging*, vol. 37, no. 11, pp. 2514–2525, 2018.
- [12] L. Huang, R. Han, T. Ai, P. Yu, H. Kang, Q. Tao, *et al.*, “Serial quantitative chest ct assessment of covid-19: Deep-learning approach,” *Radiology: Cardiothoracic Imaging*, vol. 2, no. 2, p. e200075, 2020.
- [13] L. Sun, Z. Mo, F. Yan, L. Xia, F. Shan, Z. Ding, *et al.*, “Adaptive feature selection guided deep forest for covid-19 classification with chest ct,” *IEEE Journal of Biomedical and Health Informatics*, vol. 24, no. 10, pp. 2798–2805, 2020.
- [14] K. Zhang, X. Liu, J. Shen, Z. Li, Y. Sang, X. Wu, *et al.*, “Clinically applicable ai system for accurate diagnosis, quantitative measurements, and prognosis of covid-19 pneumonia using computed tomography,” *Cell*, 2020.
- [15] Z. Wang, Q. Liu, and Q. Dou, “Contrastive cross-site learning with re-designed net for covid-19 ct classification,” *IEEE Journal of Biomedical and Health Informatics*, vol. 24, no. 10, pp. 2806–2813, 2020.
- [16] X. Ouyang, J. Huo, L. Xia, F. Shan, J. Liu, Z. Mo, *et al.*, “Dual-sampling attention network for diagnosis of covid-19 from community acquired pneumonia,” *IEEE Transactions on Medical Imaging*, 2020.
- [17] Y. Wang, Y. Zhang, Y. Liu, J. Tian, C. Zhong, Z. Shi, *et al.*, “Does non-covid19 lung lesion help? investigating transferability in covid-19 ct image segmentation,” *arXiv preprint arXiv:2006.13877*, 2020.
- [18] V. Cheplygina, M. de Bruijne, and J. P. Pluim, “Not-so-supervised: a survey of semi-supervised, multi-instance, and transfer learning in medical image analysis,” *Medical Image Analysis*, vol. 54, pp. 280–296, 2019.
- [19] N. Tajbakhsh, L. Jeyaseelan, Q. Li, J. N. Chiang, Z. Wu, and X. Ding, “Embracing imperfect datasets: A review of deep learning solutions for medical image segmentation,” *Medical Image Analysis*, p. 101693, 2020.
- [20] J. E. Van Engelen and H. H. Hoos, “A survey on semi-supervised learning,” *Machine Learning*, vol. 109, no. 2, pp. 373–440, 2020.
- [21] Z. Ji, Y. Shen, C. Ma, and M. Gao, “Scribble-based hierarchical weakly supervised learning for brain tumor segmentation,” in *International Conference on Medical Image Computing and Computer-Assisted Intervention*. Springer, 2019, pp. 175–183.
- [22] R. Huang, Y. Zheng, Z. Hu, S. Zhang, and H. Li, “Multi-organ segmentation via co-training weight-averaged models from few-organ datasets,” in *International Conference on Medical Image Computing and Computer-Assisted Intervention*. Springer, 2020, pp. 146–155.
- [23] J. Zhang, Y. Xie, Y. Xia, and C. Shen, “Dodnet: Learning to segment multi-organ and tumors from multiple partially labeled datasets,” *arXiv preprint arXiv:2011.10217*, 2020.
- [24] F. Shan, Y. Gao, J. Wang, W. Shi, N. Shi, M. Han, *et al.*, “Lung infection quantification of covid-19 in ct images with deep learning,” *arXiv preprint arXiv:2003.04655*, 2020.
- [25] A. Amyar, R. Modzelewski, H. Li, and S. Ruan, “Multi-task deep learning based ct imaging analysis for covid-19 pneumonia: Classification and segmentation,” *Computers in Biology and Medicine*, p. 104037, 2020.
- [26] C. Zheng, X. Deng, Q. Fu, Q. Zhou, J. Feng, H. Ma, *et al.*, “Deep learning-based detection for covid-19 from chest ct using weak label,” *medRxiv*, 2020.
- [27] D.-P. Fan, T. Zhou, G.-P. Ji, Y. Zhou, G. Chen, H. Fu, *et al.*, “Inf-net: Automatic covid-19 lung infection segmentation from ct images,” *IEEE Transactions on Medical Imaging*, 2020.
- [28] G. Wang, X. Liu, C. Li, Z. Xu, J. Ruan, H. Zhu, *et al.*, “A noise-robust framework for automatic segmentation of covid-19 pneumonia lesions from ct images,” *IEEE Transactions on Medical Imaging*, vol. 39, no. 8, pp. 2653–2663, 2020.
- [29] Q. Yao, L. Xiao, P. Liu, and S. K. Zhou, “Label-free segmentation of covid-19 lesions in lung ct,” *arXiv preprint arXiv:2009.06456*, 2020.
- [30] V. Chouhan, S. K. Singh, A. Khamparia, D. Gupta, P. Tiwari, C. Moreira, *et al.*, “A novel transfer learning based approach for pneumonia detection in chest x-ray images,” *Applied Sciences*, vol. 10, no. 2, p. 559, 2020.
- [31] T. Majeed, R. Rashid, D. Ali, and A. Asaad, “Covid-19 detection using cnn transfer learning from x-ray images,” *medRxiv*, 2020.
- [32] S. Misra, S. Jeon, S. Lee, R. Managuli, I.-S. Jang, and C. Kim, “Multi-channel transfer learning of chest x-ray images for screening of covid-19,” *Electronics*, vol. 9, no. 9, p. 1388, 2020.
- [33] O. Ronneberger, P. Fischer, and T. Brox, “U-net: Convolutional networks for biomedical image segmentation,” in *International Conference on Medical Image Computing and Computer-Assisted Intervention*. Springer, 2015, pp. 234–241.
- [34] Ö. Çiçek, A. Abdulkadir, S. S. Lienkamp, T. Brox, and O. Ronneberger, “3d u-net: learning dense volumetric segmentation from sparse annotation,” in *International Conference on Medical Image Computing and Computer-Assisted Intervention*. Springer, 2016, pp. 424–432.
- [35] Q. Liu, L. Yu, L. Luo, Q. Dou, and P. A. Heng, “Semi-supervised medical image classification with relation-driven self-ensembling model,” *IEEE Transactions on Medical Imaging*, 2020.
- [36] L. Gatys, A. Ecker, and M. Bethge, “A neural algorithm of artistic style,” *Journal of Vision*, vol. 16, no. 12, pp. 326–326, 2016.
- [37] Q. Dou, H. Chen, Y. Jin, L. Yu, J. Qin, and P.-A. Heng, “3d deeply supervised network for automatic liver segmentation from ct volumes,” in *International Conference on Medical Image Computing and Computer-Assisted Intervention*. Springer, 2016, pp. 149–157.
- [38] J. Ma, Y. Wang, X. An, C. Ge, Z. Yu, J. Chen, *et al.*, “Towards data-efficient learning: A benchmark for covid-19 ct lung and infection segmentation,” *Medical physics*, 2020.
- [39] A. L. Simpson, M. Antonelli, S. Bakas, M. Bilello, K. Farahani, B. Van Ginneken, *et al.*, “A large annotated medical image dataset for the development and evaluation of segmentation algorithms,” *arXiv preprint arXiv:1902.09063*, 2019.
- [40] A. Paszke, S. Gross, F. Massa, A. Lerer, J. Bradbury, G. Chanan, *et al.*, “Pytorch: An imperative style, high-performance deep learning library,” in *Advances in Neural Information Processing Systems*, 2019, pp. 8026–8037.
- [41] F. Isensee, P. F. Jaeger, S. A. Kohl, J. Petersen, and K. H. Maier-Hein, “nnu-net: a self-configuring method for deep learning-based biomedical image segmentation,” *Nature Methods*, pp. 1–9, 2020.
- [42] P. An, S. Xu, S. A. Harmon, E. B. Turkbey, T. H. Sanford, A. Amalou, *et al.* (2020) CT Images in Covid-19 [Data set]. [Online]. Available: <https://wiki.cancerimagingarchive.net/display/Public/CT+Images+in+COVID-19>